DESIGN AND ELECTROMAGNETIC MODELING OF INTEGRATED LC FILTER IN A BUCK CONVERTER

Bensaci Ahmed[1], Guettaf Yacine[2], Djekidel Rabah[1], Hamid M-H-A[3]

[1]LACoSERE laboratory, Amar Telidji University, Laghouat, Algeria
[2]Laboratory of Instrumentation and Advanced Materials,
University Center Nour Bachir of El Bayadh, Algeria
[3]University of Lorraine, CRAN, UMR 7039, France

Abstract. *This paper presents the design and electromagnetic modeling of a new structure of integrated low-pass LC filter in a buck converter. This micro-filter consists of a planar circular coil placed between two Mn-Zn ferrite substrates. Mn-Zn ferrite has been chosen because of its high permeability and permittivity. In this micro-filter substrates act not only as a magnetic core but also as a capacitor. A modelling of the electromagnetic and electric behavior of the integrated filter, we have simulated with the help of the software PSIM 9.0 on the equivalent electrical circuit of the dimensioned filter. A visualization of the different electromagnetic phenomena that appear during the operation of the filter is determined in 3D space dimension using the finite element method.*

Key words: *Converter DC-DC, COMSOL 3.5a, LC filter, modeling, Mn-Zn ferrite, Integration, PSIM 9.0*

1. INTRODUCTION

The integration of passive components for DC-DC converters applications is still a challenging area of research. The integration of planar LC passive components such as inductance and capacitance has been applied for many years [1]. These idea of integrating passive components into the converter's structure had been suggested starting in the early 1990s by a power electronics group Van Wyk nd Ferreira from the Rand Laboratory for Energy and University of South Africa. The main objective is to obtain multifunctional and compact integrated modules using conductive, dielectric, and magnetic materials with different properties, such as high conductivity, high permittivity, and high permeability. In the present work, we have chosen the Mn-Zn ferrite because of its high permeability and permittivity. In this filter Mn-Zn substrates act not only as a magnetic core but also as a capacitor. In order to reduce the conduction losses in the part of the ferrite used as a capacitor.

They are associated with a wide range of substrates, including PCBs and standard ceramic. This technology was used only for low power ranges (a few watts) for operating frequencies up to several GHz [2,3]. The filter who to be studied in this work is based on this technology but it is designed for low power range and lowest operating frequency: few watts and 100 kHz. In this paper, we present the design of an integrated output LC filter dedicated to DC-DC converters, based on use a ferrite magnetic circuit and simultaneously as a dielectric substrate for the capacitive effect. These two properties allow the conception of a hybrid LC component operating as a low pass filter. In taking into account the electric and magnetic characteristics of the materials selected, the proposed structure is composed of a planar micro-coil circular turns taken sandwiched between two ferrite layers. The outer surfaces of the ferrites are metalized to form ground planes. The operation of the micro-filter is simulated using software of type circuit (PSIM) to evaluate the performance of this model. Finally, we visualized the different electromagnetic phenomena that appear during the operation of the microfilter. It is about the distribution of the electric potential and the density of the lines of the magnetic field.

2. PRESENTATION OF THE BUCK CONVERTER

The converter is the starting point of the design of the micro-filter. We have chosen a buck converter (Fig. 1). The micro-filter we want to integrate into a buck converter will thus be dimensioned for this type of application. Input voltage, $V_{in}=5V$. The output voltage, $V_{out}=3.3V$. Output power, $P_{out}=10W$. The frequency of operation, $f=100\ kHz$.

The buck converter circuit for this circuit is shown in Fig. 1. The micro-filter to realize are two of the intrinsic elements of this converter [4-9].
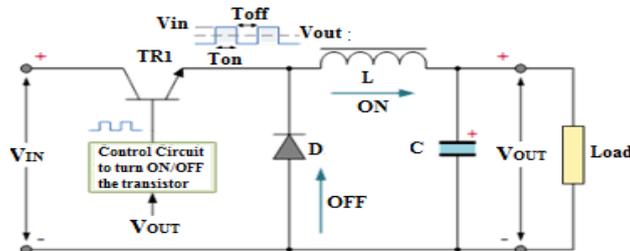
Fig. 1 Output LC low-pass filter to be used in a Buck converter

3. LC FILTER STRUCTURE

The micro-filter consists of a planar circular spiral coil sandwiched between two ferrite substrates (Figs. 2 and 3). This structure shows both inductance and distributed capacitance between the coil and the ground planes as shown in Fig. 2(b). This structure acts as an electromagnetically integrated LC low-pass filter, each element of the equivalent circuit model (Fig. 2(b)) has to be calculated from simulations (inductors) and measurements (capacitors) [7-9]. The spiral winding is divided into 2N-cell semicircle connected in series. Each semicircle is characterized by an equivalent self-inductance, mutual inductance, a series resistance and impedance inter-turn. Values of inductances and mutual inductances are obtained by an analytic method, inter-turn and volume capacitances are calculated from the *Mn-Zn* ferrite modeling results [9].

4. CALCULATION OF THE GEOMETRICAL AND ELECTRICAL PARAMETERS OF PLANAR INDUCTOR

By taking into account selected electrical and magnetic characteristics, we evaluate the volume of the magnetic core. This enables us to define the section on which we will put the electrical circuit of the planar spiral inductor, then we will determinate the dimensions of this circuit in order to meet the specifications of the converter in terms of magnetic storage of energy and losses in materials [6-9].
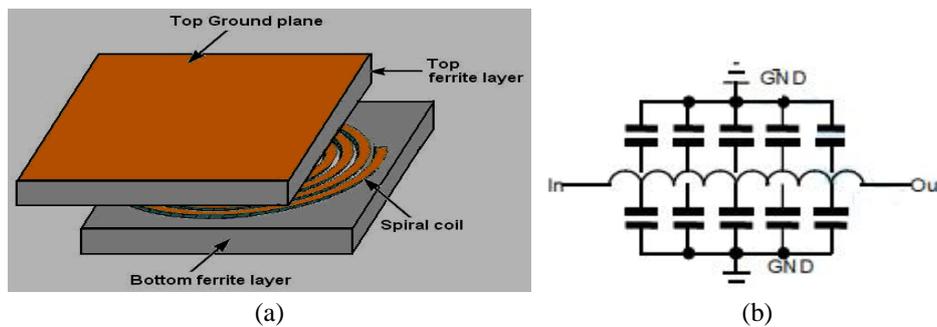
Fig. 2 (a) Exploded-view of the studied low pass filter, (b) Equivalent circuit model
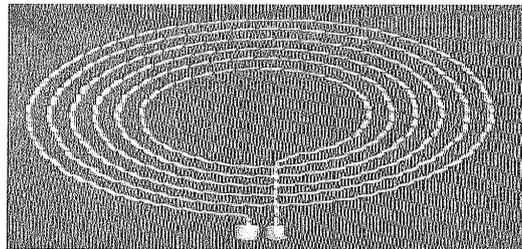
Fig. 3 Lower Mn-Zn substrate (20 Half-turn)

Each planar spiral inductor is defined geometrically by several parameters (Fig. 4) such as the number of turns n, the width of the conductor w, thickness of the conductor t, the spacing between conductor s, length of the conductor l, the outer diameter d_{out} and input diameter d_{in} [10-12].
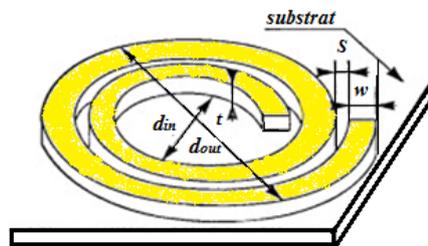
Fig. 4 Geometrical parameters of a planar spiral integrated inductor

The mathematical equations used to determine the parameters of an integrated circular spiral inductor are presented in detail in the reference [13-15]. The essential parameters are gathered in Table 1.

Table 1 Results of the dimensioning

Geometrical parameters	Results of dimensioning
Inductance: L (μH)	1,85
Number of turns: n	10
Volume of the of magnetic cores (m^3)	$615{,}25 \cdot 10^{-9}$m^3
Length of the conductor: l (mm)	583,7
Width: w (mm)	0.13
Thickness: t (mm)	0,0932
Spacing inter-turn: s (mm)	0,398
External diameter: d_{out} (mm)	19,5
Internal diameter: d_{in} (mm)	9,75

5. FILTER CIRCUIT MODEL

5.1. Modelling of Mn-Zn ferrite

The electrical properties of ferrites depend on their polycrystalline structure. The grain and insulating grain boundary are the two main components that determine the variation of resistivity and permittivity [16].

The equivalent circuit is shown in Fig. 5. R_g and R_{gb} are the grain and the grain boundary resistances respectively [7-9].
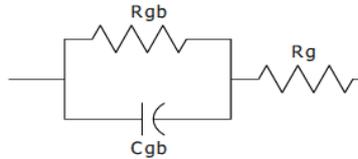
Fig. 5 Equivalent electrical circuit of Mn-Zn ferrite

Measures for extracting values of the three components of Fig. 5 were performed in the laboratory LAPLACE (Paul Sabatier University in Toulouse, France) [13]. The results are shown in Table 2.

Table 2 Fitting parameters of *Mn-Zn* at *T=20°c* (Frequency range: 10Hz-0.7MHz)

ρ_g (Ωm)	ρ_{gb} (Ωm)	ε_r
0,173	34,8	6.5×10^4

5.2. Filter model

The spiral inductor between the ferrite substrates is circular. Since the spiral inductor is a distributed structure, our proposed model is based on distributed model. Several works

have already shown that a turn may be represented by a lumped model as reported in Fig. 6 [7-9]. In order to get better accuracy, the spiral of n-turns has been broken into 2n-half-turns. The lumped model corresponds to each half-turn is represented in Fig. 6. This choice has already been preferred because in some of our studied LC filter designs the inter-turns distances vary from the input to the output filter. The overall model consists in 2n-circuits connected in series to form a distributed model. The inter-turns impedances between adjacent turns are to be considered, especially by using a high permittivity substrate [10-15].
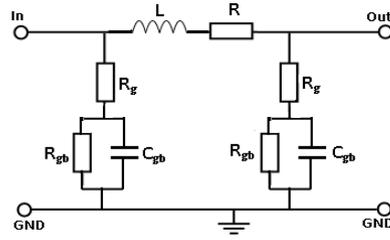
Fig. 6 Half-turn lumped model
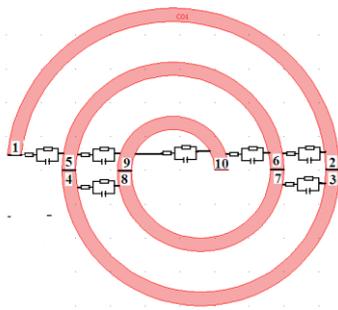
They are distributed at the front and the end of the inter-turns, leading to $2(n-1)$ inter-turns impedances. To illustrate the principle of this modeling, let us consider a LC filter with 2 turns. The resulting filter circuit model is presented in Fig. 7. The *Mn-Zn* substrate presents a high permittivity, so we did not take into account the capacitor corresponding to the air gap between two neighboring half-turns. Consequently, the capacity inter-turns of **Fig. 7** are only those due to the *Mn-Zn* substrate [7].

(a)
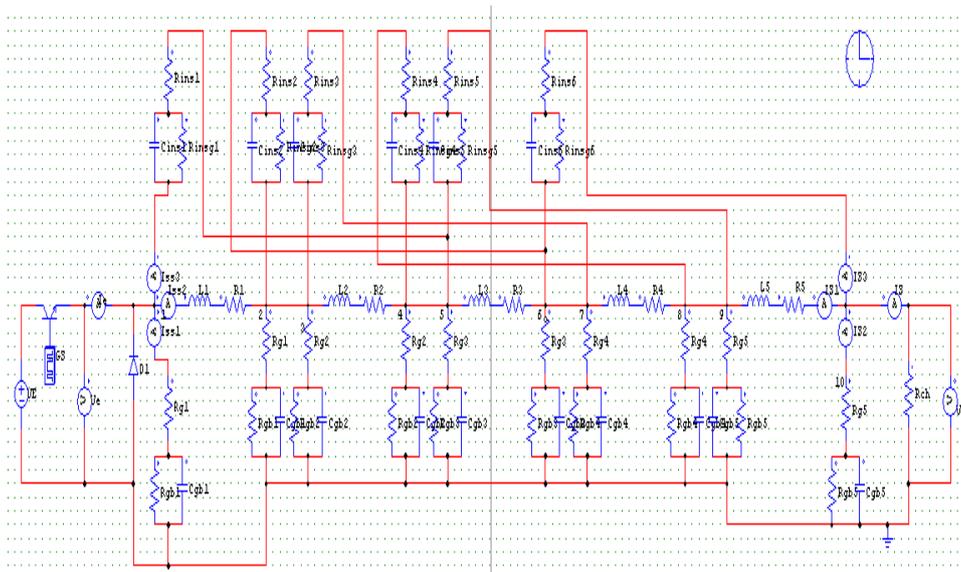
(b)

Fig. 7 2-turns filter (a) and its associated circuit model (b)

5.3. Determination of the electrical model parameters

5.3.1. Coil resistances

The resistances of each half-turn have estimated by using the following classical relationship [7-9]:

$$R_s(i) = \rho_{cu} \frac{l_{avg}(i)}{S} \tag{1}$$

With $i=1$ to n.

Where, ρ_{cu} is conductor resistivity (here copper), $l_{avg}(i)$ and S are respectively conductor mean length of each half-turn and cross-section.

$$\begin{cases} S = w \cdot t \\ l_{avg}(i) = 4 \cdot i \cdot [d_{out} - (i-1) \cdot s - i \cdot w] - s \end{cases} \tag{2}$$

5.3.2. Substrate impedances

Both resistances and capacitances of the ferrite substrates are calculated by using the fitting parameters of Table 2 [4, 5]. These relations are:

$$R_g = \rho_{gMnZn} \frac{h}{A} \tag{3}$$

$$R_{gb} = \rho_{gbMnZn} \frac{h}{A} \tag{4}$$

$$C_{gb} = \varepsilon_0 \varepsilon_{rMnZn} \frac{A}{h} \tag{5}$$

Where, h is the height of the ferrite between the half-turn and ground plane and A is the area below the half-turn of the ferrite.

5.3.3. Inter-turns impedances

The calculation of the inter-half-turn parameters is not easy. The co-planar electrodes of the tested sample have to be transformed into parallel plate electrodes by using the theory of conformal transformations developed in [17-19] (Fig. 8).

New constants are derived from the transformation as shown in the following equation [19, 20]:

$$K_R = \frac{2 \cdot K(k)}{K(K')} \quad \text{and} \quad K_C = \frac{K(k')}{2 \cdot K(k)} \tag{6}$$

Where: $K(k)$ is the complete integral of the first kind with modulus k, and $K(k')$ is the complete integral of the first kind taken in the complementary modulus k' [17-19].

The ratio $K(k)$ and $K(k')$ can be calculated from the following equation:

$$\frac{K(k')}{K(k)} = \begin{cases} \frac{1}{\pi} \cdot Ln\left(2.\frac{1+\sqrt{k'}}{1-\sqrt{k'}}\right), 0 \le k \le \frac{1}{\sqrt{2}} \\ \dfrac{\pi}{Ln\left(2 \cdot \dfrac{1+\sqrt{k}}{1-\sqrt{k}}\right)}, \frac{1}{\sqrt{2}} \le k \le 1 \end{cases} \tag{7}$$

(a)

(b)

(c)
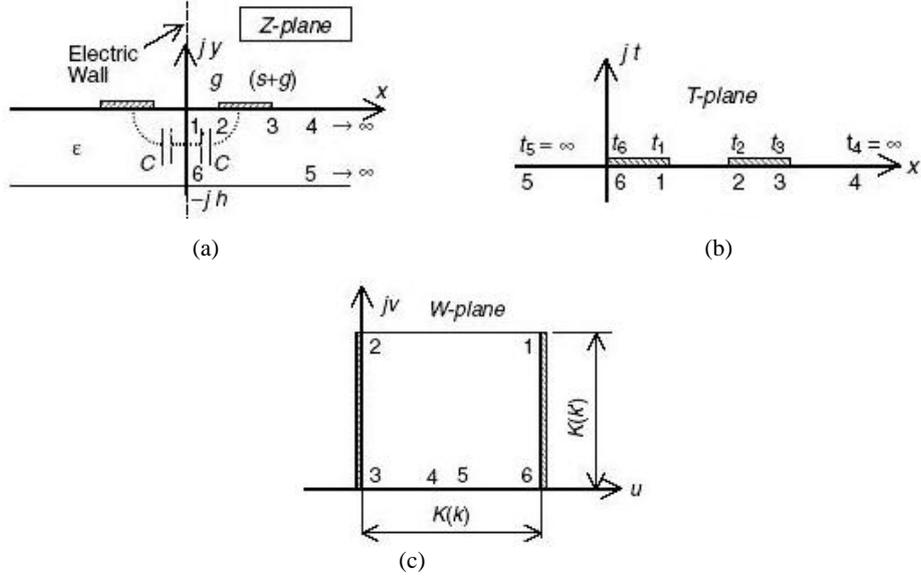
Fig. 8 Geometries of (a) two planar conductors on the upper half plane, (b) transformed conductors on the Schwarz-Christoffel rectangular region, (c) Rectangle in W-plane (the lower part of the T-plane)

So, we can calculate R'_g, R'_{gb} and C'_{gb} of inter-half-turn by using the following relationships:

$$R'_g = \rho_{gMnZn} \cdot \frac{2.K(k)}{K(k')} \cdot \frac{1}{l_{tts}(i)}$$

$$R'_{gb} = \rho_{gbMnZn} \cdot \frac{2.K(k)}{K(k')} \cdot \frac{1}{l_{tts}(i)} \tag{8}$$

$$C'_{gb} = \varepsilon_0 \varepsilon_{rMnZn} \cdot \frac{K(k')}{2.K(k)} \cdot \frac{1}{l_{tts}(i)}$$

Where, $l_{tts}(i)$ is the mean length of inter-half-turn.

$$l_{tts}(i) = 4 \cdot i \cdot [d_{out} - (i-1) \cdot w - i \cdot s] - w \tag{9}$$

All the parameters of the filter can be now computed.

6. RESULTS OF THE ELECTRICAL PARAMETERS OF THE INTEGRATED FILTER

The calculated electrical parameters of the equivalent electrical circuit of the integrated filter are shown in Table 3.

Table 3 Electrical Parameters Results

Number of turns'	The resistances and inductor of each half-turn		Substrate impedances			Inter-turns impedances			Total length
n	$R_s(\Omega)$	$L_s(\mu H)$	$R_g(\Omega)$	$R_{gb}(k\Omega)$	$C_{gb}(\mu F)$	$R_{insg}(\Omega)$	$R_{insgb}(\Omega)$	$C_{insgb}(\mu F)$	$L_t(m)$
1	0.0189	0.019	25.896	5.2122	0.0038	2.8386	571.3285	6.029	0.0771
2	0.0370	0.074	13.277	2.6725	0.0075	1.4584	293.5440	3.097	0.1503
3	0.0539	0.167	9.099	1.8315	0.0109	1.0005	201.3681	2.125	0.2194
4	0.0699	0.297	7.024	1.4138	0.0141	0.7729	155.5582	1.641	0.2842
5	0.0847	0.464	5.790	1.1654	0.0172	0.6375	128.3047	1.354	0.3448
6	0.0986	0.669	4.976	1.0017	0.0200	0.5482	110.3451	1.164	0.4011
7	0.1114	0.910	4.404	0.8864	0.0226	0.4855	97.7130	1.031	0.4532
8	0.1232	1.189	3.983	0.8017	0.0250	0.4393	88.4277	0.933	0.5011
9	0.1339	1.504	3.663	0.7374	0.0271	0.4044	81.3911	0.859	0.5448
10	0.1436	1.857	3.416	0.6876	0.0291	0.3773	75.9470	0.801	0.5843

We performed simulations in order to test the operation of our equivalent electrical circuit of the micro-filter integrated. The simulation was performed using PSIM software 9.0. In this simulation, the circuit of Fig. 7(b) contains an equivalent electrical circuit of the micro-filter.

Figs. 9 and 10 show the waveform of the output ant input voltage and current of the micro-filter. The output voltage is 4.414 *V* instead of 5 *V*. This is due to resistive losses in the conductor, then the magnetic core losses. In steady state, the current is 2.20 *A*, corresponding to 8.7 *W* output power instead of 10 *W*.
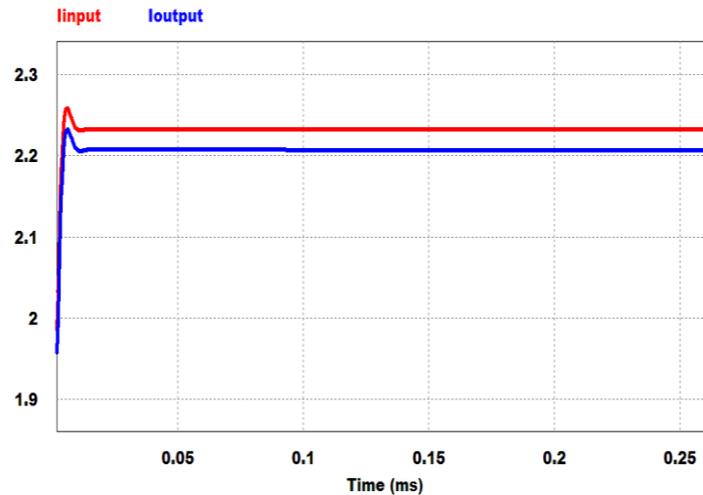
Fig. 9 Waveforms of the output and input current of the micro-filter
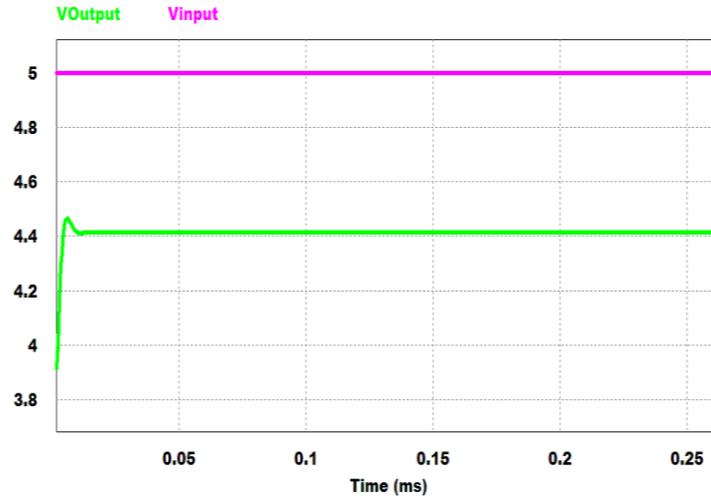
Fig. 10 Waveforms of output and input of voltages and currents of the micro-filter

The measured values of output and input of voltages and currents of the micro-filter are given in the following Tables (4 and 5):

Table 4 Measured values at the time instant $t=6.78e-005s$ of the output and input currents

	Measures
Time	$6.78e-005$
I_{Input} (A)	2.232
$I_{Output}(A)$	2.207

Table 5 Measured values at the time instant $t=6.78e-005s$ of the output and input voltages

	Measures
Time	$6.78e-005$
V_{Input} (V)	4.999
V_{Output} (V)	4.414

7. ELECTROMAGNETIC MODELING OF THE LC FILTER

In this section, we present the different electromagnetic phenomena that appear during the operation of the filter in a buck converter to see the distribution of the magnetic flux density and the electric field. This simulation was performed using the software COMSOL 3.5a.

7.1. Simulation parameters under COMSOL 3.5a

To get closer to reality and based on the results of the dimensioning as shown in Table 1, we will show the geometry of our micro filter model Designed in 3D as shown in Figure 11.
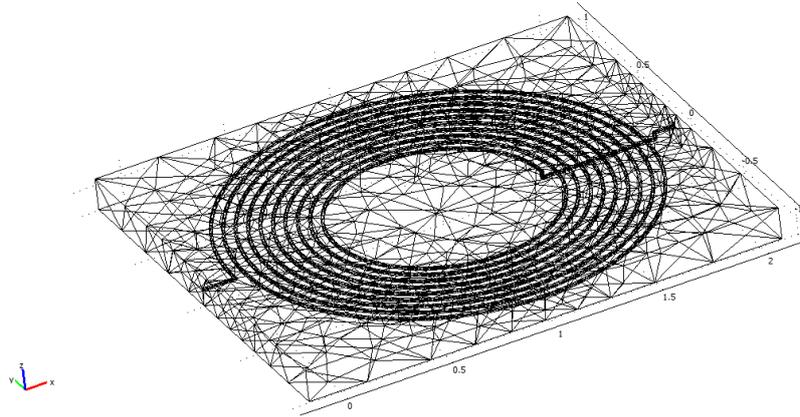
Fig. 11 Structure of the micro-filter simulated with the mesh of the field of study

In Table 6 we group together the simulation parameters used. This is to define the mesh: number of nodes and type of elements. We have also noted the simulation time.

Table 6 Simulation parameters

Number of elements of the mesh		Type of	Execution time	Core volume
spiral	substrate	elements	(s)	(m^3)
7766	40486	Tetrahedral	2032,372	669,60.10^{-9}

7.2. Simulation results

Figs. 12, 13 and 14 show the distribution of the electric potential in the LC filter. We note in Fig. 12 that the distribution of potential is in adequacy with the specifications. Indeed, for a current injected of *2 A*, the potential takes the greatest value at the input of the micro-filter ($\approx$ 3.5 V), then decreases until reaching the value of 2 *V*.
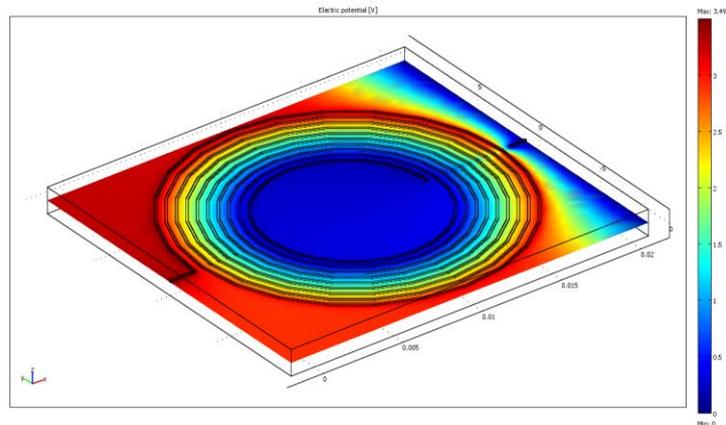
Fig. 12 Distribution of the electric potential in the micro filter

Fig. 13 shows that in the half-turns of the micro filter, located in the right half in this figure, of the falls of potential generated by the different losses at the ferrite (substrate). These losses decrease as one approach the exit of the micro filter. Indeed, in this zone, the parasitic effects are almost non-existent.
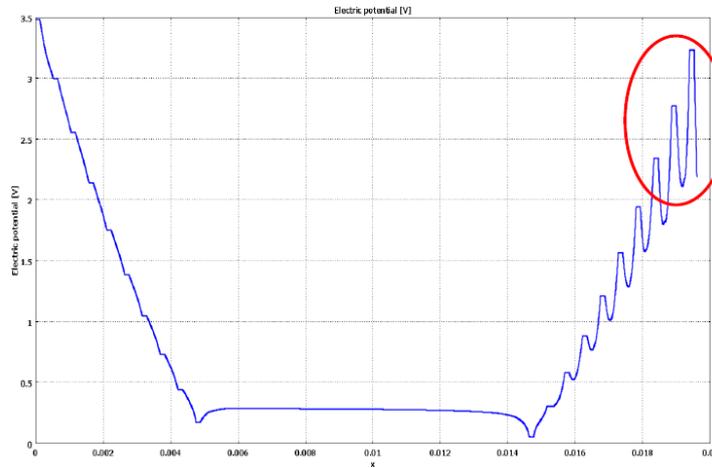
Fig. 13 Variation of the electric potential in the micro filter

Fig. 14 shows the distribution of the lines of magnetic field in our micro filter. These lines of field are concentrated at the input of the micro filter because of the high value of the current in this region. On the other hand, the majority of these lines of field are confined in a substrate because of high permeability of ferrite.
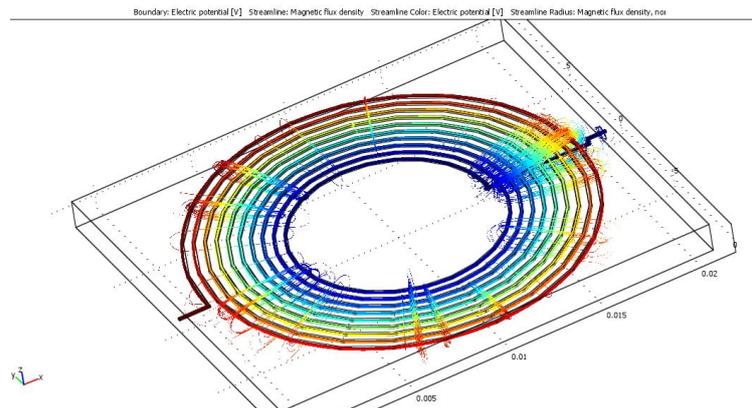
Fig. 14 Distribution of the lines of magnetic field of the micro filter

Figs. 15 (a, b, and c) shows a good vertical propagation of the field in the material. The work frequency not being high enough, the eddy currents are not thus yet sufficiently important to modify the distribution of the lines of field.

(a)

(b)

(c)
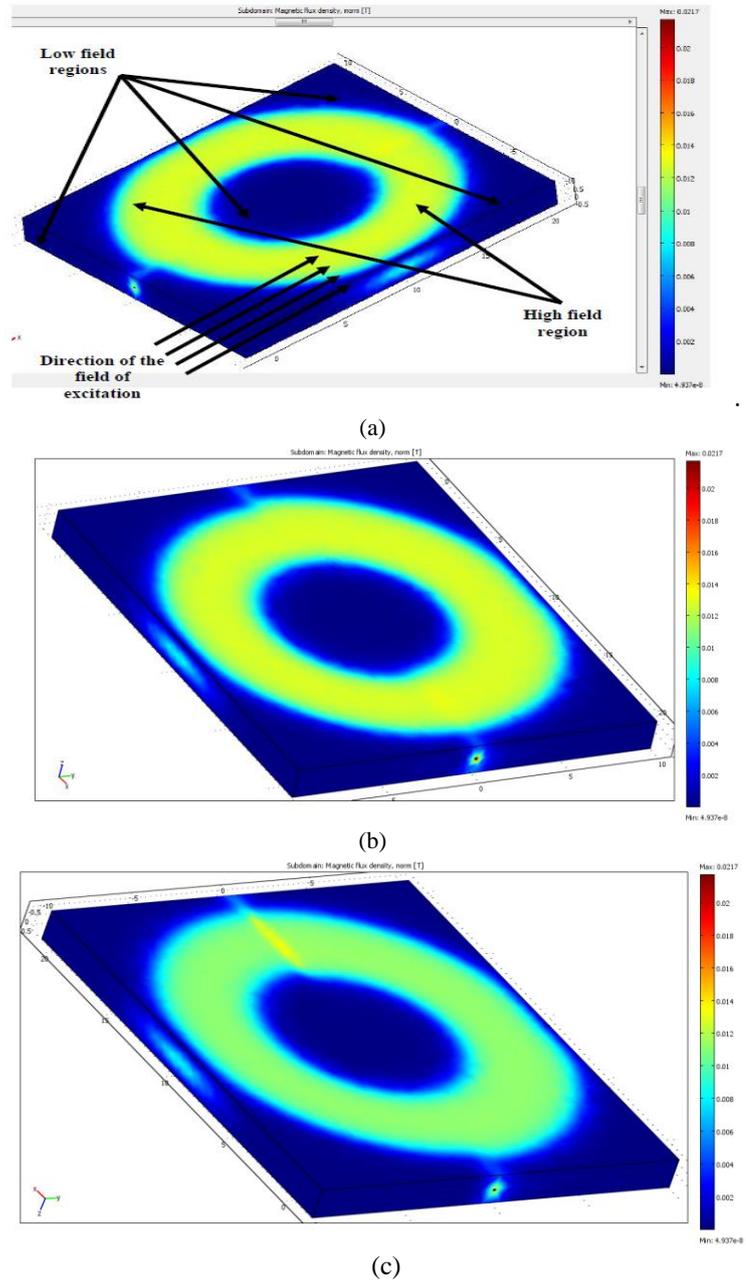
Fig. 15 Distribution of the density flux magnetic in the micro filter (a) Different direction
of the lines of field, (b) magnetic flux on the upper part of the micro filter,
(c) magnetic flux on the lower part of the micro filter

Fig. 16 gives an overview of the distribution of the density of the magnetic flux in the micro filter. Because of the distribution of the current in the conductor, this last being more important in the right half of the micro coil, the density of flow is some more important.
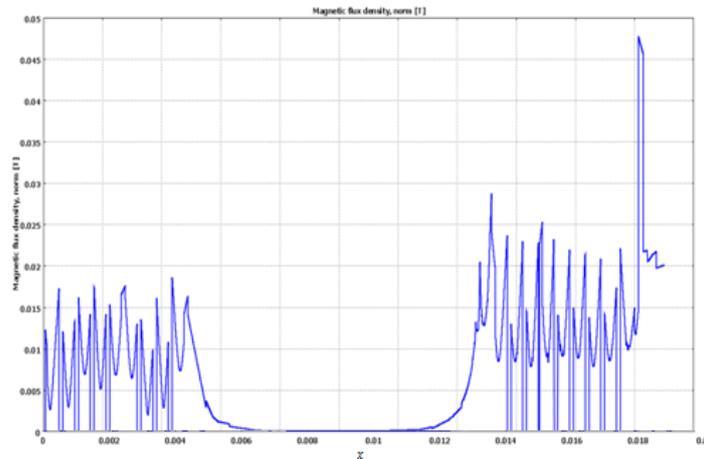
Fig. 16 Variation of the density of the magnetic flux in the micro filter

8. CONCLUSIONS

In this paper, we have presented the dimensioning, the modeling and the simulation of a micro filter. First, we have calculated the geometrical and electrical parameters of planar inductor. Then, we have proposed a new structure of the micro filter consists in a planar spiral coil sandwiched in between two ferrite substrates. This structure shows both distributed capacitance and inductance between the spiral and the ground planes. Next, we have used *Mn-Zn* ceramic substrates in this work for both their high permeability and permittivity. Already largely used as core material, the goal of this study was to show that *Mn-Zn* may also be used as a capacitor in a DC-DC power converter integrated LC filter. Next, by using a software simulation PSIM 9.0, we have compared the waveforms of the converter output voltages.

Finally, by using the software COMSOL 3.5a, we have visualized the distribution of the lines of field of our micro filter in order to know if they do not overflow and thus do not disturb the other elements of the converters. We also visualized the density of the magnetic flux and the electric potential. We conclude that the results of dimensioning in this paper are interesting indeed.

REFERENCES

[1]   Ph. Artillan, M. Brunet, D. Bourrier, J-P. Laur, N. Mauran, "Integrated LC filter on silicon for DC-DC converter applications", *IEEE Transactions on Power Electronics, Institute of Electrical and Electronics Engineers*, vol.26, no. 8, pp. 2319–2325, 2011

[2]   J. D. Van-Wyk, F. C. Lee, Z. Liang, R. Chen, S. Wang, B. Lu, "Integrating Active, Passive and EMI-Filter Functions in Power Electronics Systems: A Case Study of Some Technologies", *IEEE Transactions on Power Electronics*, vol. 20, no. 3, pp. 523–536, May 2005.

[3]   M. Ali, E. Labouré, F. Costa, B. Revol, "Design of a Hybrid Integrated EMC Filter for a DC-DC Power Converter ", *IEEE Transactions on Power Electronics*, vol. 27, no. 11, pp. 4380–4390, Nov 2012.

[4]   M. Rabia, H. Azzedine, T. Lebey, "Modeling and dimensioning of a planar inductor for a monolithic integration", In Proceedings of the Asia-Pacific Power and Energy Engineering Conference IEEE, 2011, pp. 1–9.

[5]   M. Derkaoui, A. Hamid, T. Lebey, R. Melati, "Design and modeling of an integrated micro-transformer in a flyback converter", *Telkomnika journal*, vol.11, no. 4, pp. 669–682, 2013.

[6]   Y. Guettaf, A. Flitti, A. Bensaci, H. Kharbouch, M. Rizouga, A. Hamid, "Simulation of the operation of a DC–DC converter containing an inductor of planar type", *Electrical Engineering journal*, vol. 100, no. 2, pp. 953–969, June 2018.

[7]   H. H. Nien, T. J. Liang, J. F. Chen , S. K. Changchien, "Study of the Electrical and Magnetic Properties of MnZn Ferrite by Equivalent Electrical Elements", In Proceedings of the Second International conference on Innovative computing information and Control IEEE, Sept 2007.

[8]   Q. Y. Yan, R. J. Gambino, S. Sampath, "Plasma-Sprayed MnZn Ferrites with Insulated Fine Grains and Increased Resistivity for High-Frequency Applications", *IEEE Transactions on Magnetic*, vol. 40, no. 5, pp. 3346–3351, 2004.

[9]   H. H. Nien, J. F. Chen, S. K. Changchien, H.W. Shieh, "Implementation of low loss Mn-Zn Ferrite cores for power electronics applications", In Proceedings of the IEEE Power India conference, 2006.

[10] R. Melati, A. Hamid, T. Lebey, M. Derkaoui, "Design of a new electrical model of a ferromagnetic planar inductor for its integration in a micro-converter", *Mathematical and Computer Modelling*, vol. 40, no. 1-2, pp. 200–227, Jan 2013.

[11] S.S. Mohan, M. del Mar Hershenson, S.P. Boyd, T.H. Lee, "Simple accurate expressions for planar spiral inductances", *IEEE Journal of Solid-State Circuits*, vol. 34, no. 10, pp. 1419–1424, Oct 1999.

[12] Y. Benhadda, A. Hamid, T. Lebey, "Thermal Modeling of an Integrated Circular Inductor", *Journal of Nano- and Electronic Physics*, vol. 9, no. 1, pp. 01004 (5pp), 2017.

[13] A. Bensaci, A. Hamid, A. Flitti, T. Lebey, V. Bley, F. Z. Medjaoui, "Design of a New Electrical Model of Integrated LC Filter in DC–DC Converter", *Journal of Low Power Electronics*, vol. 12, no. 1, pp. 34–44, 2015.

[14] I. Kowase, T. Sato, K. Yamasawa, Y. Miura, "A Planar Inductor Using Mn–Zn Ferrite/Polyimide Composite Thick Film for Low-Voltage and Large-Current DC–DC Converter", *IEEE Transactions on Magnetics*, vol. 41, no. 10, pp. 3991–3993, Oct 2005.

[15] B. Rejaei, "Mixed-Potential Volume Integral-Equation Approach for Circular Spiral Inductors", *IEEE Transactions on Microwave Theory and Techniques*, vol. 52, no. 8, pp. 1820–1829, Aug 2004.

[16] Y.Katayama, S. Sugahara, H. Nakazawa, E. Masaharu, "High-Power-Density MHz Switching Monolithic DC-DC converter with Thin-Film Inductor", *IEEE Power Electronics Specialists Conference*, vol. 3, pp.1485–1490, Jun 2000.

[17] S. Gevorgian, H. Berg, H. Jacobsson, T. Lewin , "Basic Parameters of Coplanar-Strip Waveguides on Multilayer Dielectric/semiconductor Substrate, Part1: High Permittivity Superstrates", *IEEE microwave magazine*, vol.4, no. 2, pp. 60–70, Jun 2003.

[18] J. D. Van-Wyk, F. C. Lee, Z. Liang, R. Chen, S. Wang, B. Lu , " Integrating Active, Passive and EMI-Filter Functions in Power Electronic System: A Case Study of Some Technologies", *IEEE Transactions on Power Electronics*, vol. 20, no. 3, pp. 523–536, May 2005.

[19] C. J. Nassar, C. A. Kosik-Williams, D. Dawson-Elli, R. John- Bowman, "Thin film CMOS on glass: The behavior of enhancement mode PMOSFETs from cutoff through accumulation", *IEEE Transactions on Electron devices*, vol. 56, no. 9, pp. 1974–1979, Sept. 2009.

[20] S. Gevorgian, H. Berg, "Line capacitance and impedance of coplanar-strip waveguides on substrates with multiple dielectric layers", In Proceedings of the 1st European Microwave Conference, September 2001, pp. 153–156.